

Trileucine and Pullulan Improve Anti-*Campylobacter* Bacteriophage Stability in Engineered Spray-Dried Microparticles

*Nicholas B. Carrigy^a, Lu Liang^b, Hui Wang^a, Samuel Kariuki^c, Tobi E. Nagel^d, Ian F.
Connerton^b, Reinhard Vehring^{a*}*

5 ^a Department of Mechanical Engineering, University of Alberta, Edmonton, Canada

^b School of Biosciences, University of Nottingham, Loughborough, UK

^c Centre for Microbiology Research, Kenyan Medical Research Institute, Nairobi, Kenya

^d Phages for Global Health, Oakland, USA

* Corresponding Author

10 Prof. Reinhard Vehring

University of Alberta, Department of Mechanical Engineering

10-203 Donadeo Innovation Centre for Engineering

9211 116th Street NW, Edmonton, Alberta, T6G 1H9, Canada

Telephone: +1 780 492 5180

15 Fax: +1 780 492 2200

E-mail: reinhard.vehring@ualberta.ca

Running header: Trileucine and pullulan stabilize spray-dried phage

ABSTRACT

20 Spray drying biologics into a powder can increase thermal stability and shelf-life relative to liquid formulations, potentially eliminating the need for cold chain infrastructure for distribution in developing countries. In this study, process modelling, microparticle engineering, and a supplemented phase diagram were used to design physically stable fully amorphous spray-dried powder capable of stabilizing biological material. A greater
25 proportion of anti-*Campylobacter* bacteriophage CP30A remained biologically active after spray drying using excipient formulations containing trehalose and a high glass transition temperature amorphous shell former, either trileucine or pullulan, as compared to the commonly used crystalline shell former, leucine, or a low glass transition temperature amorphous shell former, pluronic F-68. Particle formation models suggest that the
30 stabilization was achieved by protecting the bacteriophages against the main inactivating stress, desiccation, at the surface. The most promising formulation contained a combination of trileucine and trehalose for which the combined effects of feedstock preparation, spray drying, and 1-month dry room temperature storage resulted in a titer reduction of only $0.6 \pm 0.1 \log_{10}(\text{PFU mL}^{-1})$. The proposed high glass transition temperature amorphous
35 formulation platform may be advantageous for stabilizing biologics in other spray drying applications in the biomedical engineering industry.

Key Terms: amorphous shell former platform, *Campylobacter jejuni*, glass transition temperature, global health, *Myoviridae* phage CP30A, particle engineering, process model, shelf-life, spray drying, supplemented phase diagram

40 INTRODUCTION

Spray drying is a one-step continuous process for converting liquid containing dissolved or suspended solids into a dry powder by solvent evaporation of the atomized liquid in a hot drying gas. The removal of the solvent, typically water, decreases water-mediated degradation, improves thermal stability, and decreases weight and volume.³ These
45 improvements allow for more effective shipping, handling, and storage.³⁰ For these reasons, spray drying is widely used in the food, pharmaceutical, chemical, and mining industries, among others.^{1,2,17} In comparison, the main alternative process for generating dry powder, lyophilization, is a batch process that requires more time, is higher cost, and typically requires a secondary milling step if particle size adjustment is needed.^{22,23} Improvements to
50 spray drying techniques for stabilizing biological materials are of increasing interest for applications in the biopharmaceutical industries, where stabilized biologics are widely used as vaccines and for the treatments of common chronic illnesses such as arthritis and diabetes.²⁹

We recently applied spray drying to stabilize bacteriophages (phages) active against
55 *Campylobacter jejuni*,⁴ a leading cause of foodborne illness worldwide and a relatively major source of childhood mortality in Kenya.¹⁹ A limitation of the study was the extent of phage inactivation that occurred due to desiccation during spray drying.⁴ Biological inactivation by desiccation may be due to loss of hydrogen bonds, resulting in irreversible protein denaturation. The desiccation effect is strongest at the surface of the drying droplets, which
60 is where biologics tend to concentrate during spray drying and exposure to drying gas occurs during particle formation.^{3,4} Therefore, it is hypothesized that excipients that increase viscosity and solidify into an amorphous solid phase early during the drying process may be capable of limiting the exposure of the biologic to the drying gas and may allow for

hydrogen bond replacement to counter desiccation stress. However, under normal spray
65 drying conditions, the commonly used shell forming excipient, leucine, crystallizes,⁸ and
therefore is incapable of providing stabilization in an amorphous glass. Thus, testing the
ability of shell forming excipients that can provide glass stabilization to spray-dried biologics
is of interest. Two such excipient options are trileucine and pullulan.

Trileucine is a tripeptide that has been used to produce low-density and non-cohesive
70 particles.¹⁵ It does not crystallize under typical spray drying conditions and has a sufficiently
high dry glass transition temperature, ~104°C, a low solubility in water, and a high surface
activity,^{15,27} typically resulting in early solidification during the evaporation of aqueous
solution droplets. These are favourable properties for minimizing exposure of phages to the
drying gas.

75 Pullulan is an extracellular linear polysaccharide that has been used to produce respirable
microparticles.⁵ It has a very high dry glass transition temperature of ~261°C and a high
molecular mass.^{5,7,24-25} Since pullulan diffuses slowly due to its high molecular mass, it tends
to quickly enrich and increase viscosity near the surface of drying droplets,⁵ leading to early
shell formation and potentially the prevention of phages from exposure to desiccation
80 stress at the surface of the forming microparticles.

In this study, trileucine and pullulan, as amorphous shell formers, were compared to leucine
and a polymeric surfactant, for improving the biological stability of spray-dried phages. This
was tested using anti-*Campylobacter* phage CP30A as a model biologic and trehalose as a
bulk stabilizing agent. The inactivation during processing and the short-term biological and
85 physical storage stability of the powder without refrigeration were tested. The latter is
important for use in developing countries without cold chain infrastructure. A process
model and a supplemented phase diagram were applied to select spray drying parameters

suitable for producing stable phage powder. Microparticle engineering models were used in particle design and particle formation models assisted in explaining the mechanisms of biological stabilization.

MATERIALS AND METHODS

Phage CP30A

Phage CP30A is a *Myoviridae* that infects *Campylobacter jejuni*. The phage generation and assay were described in detail in a previous study.⁴ In this study, after the amplified lysate was 0.22 μm filtered, it was further purified by centrifugation and pellet resuspension in water, and 1:100 dilution into formulation, which was found to improve biological stability in our previous study.⁴

Formulation

To achieve the stabilization of biologics by amorphous shell formation, the dissolved solids concentration of trileucine in the feed solution was chosen to be near the solubility limit¹⁵ of $\sim 6.8 \text{ mg mL}^{-1}$. This allows for the development of rugose microparticles that solidify early in the drying process to encapsulate the phages. For pullulan, the dissolved solids concentration was chosen to be high enough to ensure early solidification, but not so high that it would increase viscosity to the point that atomization was affected.⁵ Pluronic F-68 surfactant, which has a low glass transition temperature of -63°C ,¹² was tested at the same dissolved solids concentration as trileucine, as it has a similar surface activity at this concentration, and the mass fraction is the same, making results comparable. Leucine and trehalose were tested at the same dissolved solids concentration used previously to examine shipping stability without cold chain infrastructure.⁴

110 Accordingly, the following aqueous formulations were prepared and tested with phages: (1)
4 mg mL⁻¹ trileucine (Product no. L0879, lot BCBP2254V; Sigma-Aldrich, St. Louis, MO, USA)
and 100 mg mL⁻¹ D-(+)-trehalose dihydrate (Cat. no. BP2687; Fisher BioReagents, NH, USA);
(2) 20 mg mL⁻¹ pullulan (Product no. J66961, lot N21D031; Alfa Aesar, Tewksbury, MA, USA)
and 100 mg mL⁻¹ trehalose; (3) 4 mg mL⁻¹ pluronic F-68 (Product no. P7061, lot
115 70M011718V; Sigma-Aldrich, St. Louis, MO, USA) surfactant and 100 mg mL⁻¹ trehalose; (4)
20 mg mL⁻¹ L-leucine (Code 125121000, lot A0269620; Acrōs Organics, NJ, USA) and 100 mg
mL⁻¹ trehalose. Control measurements were performed using 100% pullulan at 20 mg mL⁻¹
and 100% trehalose at either 30 mg mL⁻¹ or 100 mg mL⁻¹.

Spray Dryer Process Modelling

120 The spray dryer used in this study was a Büchi B-191 (Büchi Labortechnik AG, Flawil,
Switzerland) with a custom twin-fluid atomizer that has been described in detail previously.⁴
A mechanistic process model based on steady state heat and mass balances on the spray
dryer, similar to previous work,³ was used to determine suitable conditions for processing
and storing the phage powder. First, the inlet processing conditions were used to predict
125 the outlet conditions. Then, the moisture content in the powder at the outlet was predicted.
The plasticized glass transition temperature was then predicted and compared to the
storage target.

At constant pressure, the change in enthalpy, h , between two locations, 'in' and 'out', for an
incompressible liquid or ideal gas, is given by,³

$$h_{\text{out}} - h_{\text{in}} = c_p (T_{\text{out}} - T_{\text{in}}) \quad (1)$$

130 where T is temperature and c_p is specific heat capacity.

Steady state conditions were assumed. Figure 1 shows a control volume around the spray dryer with process model parameters used for the energy balance.

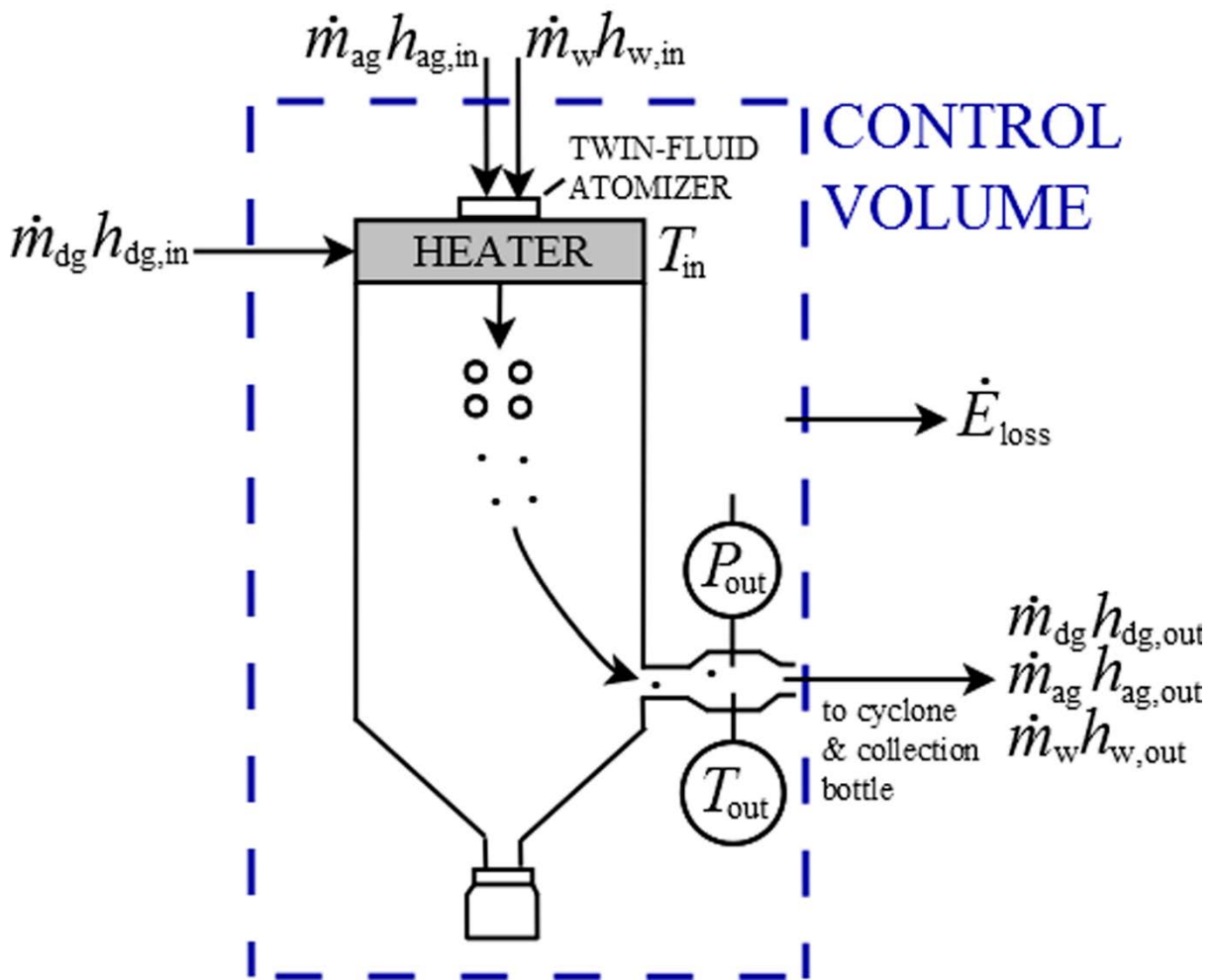


Figure 1: Thermodynamic control volume around the spray dryer and associated process

135 model parameters. Notation: \dot{E}_{loss} = energy (heat) loss from the spray dryer; \dot{m}_{dg} = drying
 gas mass flow rate; \dot{m}_{ag} = atomizing gas mass flow rate; \dot{m}_w = solvent (water) mass flow
 rate; h_{dg} = enthalpy of drying gas; h_{ag} = enthalpy of atomizing gas; h_w = enthalpy of solvent;

P_{out} = outlet pressure; T_{in} = inlet temperature; T_{out} = outlet temperature.

The energy change of the atomizing gas, $\dot{m}_{ag}(h_{ag,out} - h_{ag,in})$, was found to be negligible.

140 Additionally, the sensible heat change of the solvent was negligible; thus, only the latent
 heat of evaporation was considered for the solvent. The effects of energy changes of the

solute and the formed solid were also neglected. Applying an energy balance on the control volume with these assumptions gives,

$$\dot{m}_{dg}h_{dg,in} = \dot{E}_{loss} + \dot{m}_{dg}h_{dg,out} + \dot{m}_w\Delta h_{w,evap} \quad (2)$$

where \dot{m} is mass flow rate, the subscript 'dg' refers to drying gas and 'w' to the solvent: water here. The term \dot{E}_{loss} refers to energy (heat) loss from the spray dryer, which is not
145 adiabatic.

Rearranging equation (2) and using equation (1) gives,

$$\dot{E}_{loss} = \dot{m}_{dg}c_{p,dg}(T_{in} - T_{out}) - \dot{m}_w\Delta h_{w,evap} \quad (3)$$

An empirical linear relation for heat loss is given by,

$$\dot{E}_{loss} = \alpha T_{out} + \beta \quad (4)$$

where the constants α and β were experimentally determined by fitting data obtained using
150 different inlet temperatures (range 50 - 80°C), liquid feed flow rates (range 0 - 3.3×10⁻⁵ kg s⁻¹), and drying gas flow rates (range 4.5×10⁻³ - 1.0×10⁻² kg s⁻¹).

Substituting and isolating for outlet temperature gives,³

$$T_{out} = \frac{(\dot{m}_{dg}c_{p,dg}T_{in} - \dot{m}_w\Delta h_{w,evap} - \beta)}{(\dot{m}_{dg}c_{p,dg} + \alpha)} \quad (5)$$

The water activity at the outlet, a_{out} , is given by,

$$a_{out} = p_w/p_{w,sat} \quad (6)$$

where the saturation vapour pressure, $p_{w,sat}$, was found for different outlet temperatures
155 by the empirical Antoine equation,²¹ and the water vapour partial pressure, p_w , is,³

$$p_w = \frac{p_{out} \times (\dot{m}_w/M_w)}{(\dot{m}_w/M_w) + (\dot{m}_{dg}/M_{dg})} \quad (7)$$

where p_{out} is the outlet pressure and M refers to molecular mass.

The outlet water activity was used to predict moisture content in the powder using literature data,²⁰ giving the following approximation for trehalose moisture uptake,

$$w_2 = 2.26 \times 10^{-3} a_{\text{out}} \quad (8)$$

where w_2 is the mass fraction of water in the trehalose powder. The moisture content was used to predict the glass transition temperature for a trehalose-water system, $T_{g,\text{mix}}$, to develop a plasticization curve using the Gordon-Taylor equation,³

$$T_{g,\text{mix}} = (w_1 T_{g,1} + K w_2 T_{g,2}) / (w_1 + K w_2) \quad (9)$$

where the glass transition temperature of trehalose, $T_{g,1} = 387$ K, and the glass transition temperature of water, $T_{g,2} = 138$ K, were used with a constant $K = 7.5$, according to literature data.⁶ The mass fraction of trehalose was assumed to be $w_1 = 1 - w_2$. Pullulan and trileucine were neglected for solid phase modelling. This is a conservative assumption as their inclusion would increase the glass transition temperature and theoretically lead to even better physical stability than predicted. The glass transition temperature and moisture content were plotted versus outlet water activity.

Supplemented Phase Diagram

A non-equilibrium supplemented phase diagram (refer to Figure 4) was developed using a method described previously³ and the equations given above. Briefly, the phase of a trehalose-water system at different temperatures and mass fractions of water was supplemented with process modelling predictions of moisture content and temperature of the droplets and produced powder throughout an approximation of the drying and storage process. The plasticization data of glass transition temperature for different moisture contents was also included. This diagram is useful for choosing processing, packaging, and stability testing conditions to ensure adequate manufacturability and physical stability,

which may be related to biological stability, as trehalose crystallization has been shown to inactivate biologics.²⁶

180 The droplets were assumed to remain near the wet bulb temperature¹⁷ and then dry into particles that quickly reach the temperature of the drying gas in their vicinity, which was approximated in the diagram. As the particles proceed through the dryer to the outlet and collection bottle, heat loss occurs from the dryer and correspondingly the powder moisture content increases because cooler air has a lower saturated vapour pressure. The storage
185 conditions were designed to be at least 50°C below the glass transition temperature at the final moisture content,¹⁰ and the packaging was designed to protect against humidity intrusion.

Raman spectroscopy was performed using a custom Raman spectrometer³¹ after the powder was stored at room temperature for 4 months in a previously developed packaging
190 system⁴ to confirm physical stability predictions from the supplemented phase diagram.

Microparticle Engineering Models and Particle Morphology

Microparticle engineering models were used to predict the evaporation time until solidification at the surface begins, the corresponding outer shell diameter, and the resulting particle morphology. Atomization causes droplets to be dispersed in hot drying gas
195 resulting in solvent evaporation that leads to recession of the droplet surface and redistribution of solute or suspended matter in the droplet by diffusion. Unless the solute or suspended matter is capable of quickly diffusing to the interior of the droplet, it will tend to increase in concentration at the surface. A common approach to model this process is to use a non-dimensional Péclet number developed under the assumptions of 1-D spherical
200 symmetry and no convection except Stefan flow.²⁸ The effects of surface activity, shell

deformation, change of droplet viscosity, and non-constant evaporation rates were not considered. The non-dimensional Péclet number of solute i is given by,²⁸

$$Pe_i = \frac{\kappa}{8D_i} \quad (10)$$

where D_i is the diffusion coefficient of solute or suspended matter, i , in the droplet solvent and κ is the evaporation rate taken as $4.0 \times 10^{-9} \text{ m}^2 \text{ s}^{-1}$ for the chosen drying conditions.²⁸ The diffusion coefficient of pullulan in water was approximated to be $2.8 \times 10^{-11} \text{ m}^2 \text{ s}^{-1}$ for a typical molecular mass of 115 kDa.¹⁸ The diffusion coefficients of trehalose and trileucine were both approximated to be $5.0 \times 10^{-10} \text{ m}^2 \text{ s}^{-1}$.²⁸ The diffusion coefficient of pluronic F-68 was approximated to be $1.0 \times 10^{-10} \text{ m}^2 \text{ s}^{-1}$ based on data for pullulan at the same molecular mass, 8.35 kDa.¹⁸

Dissolved or suspended solids with a high Péclet number diffuse slowly relative to the surface recession rate resulting in an increase in their concentration near the surface.²⁷ A low Péclet number, i.e. less than 1, results in a relatively homogeneous distribution of the dissolved or suspended solids.²⁷

The surface enrichment is defined as the ratio of surface concentration to mean concentration. A numerical model fit to the solution of Fick's second law with the previous assumptions indicated that the surface enrichment of component i may be accurately approximated by,²⁸

$$E_i = 1 + \frac{Pe_i}{5} + \frac{Pe_i^2}{100} - \frac{Pe_i^3}{4000} \quad (11)$$

Due to this surface enrichment, dissolved solids with a high Péclet number will tend to first solidify at the droplet surface, where their concentration is highest, while the interior will not solidify until later in the drying process. For multi-component amorphous systems, co-

solidification will occur at the surface of the drying droplet after evaporating for the characteristic time, $t_{t,mix}$, given by,⁵

$$t_{t,mix} = \tau_D \left[1 - \left(\sum_i E_i P_i \right)^{\frac{2}{3}} \right] \quad (12)$$

where τ_D is the droplet lifetime defined as $\tau_D = d_0^2/\kappa$, in which d_0 is the initial droplet diameter, which was assumed to be 9 μm based on data of mass median diameter for the twin-fluid atomizer and air-liquid ratio settings used,¹⁴ giving a droplet lifetime of 20 ms with the previously given evaporation rate. The non-dimensional number P_i is the ratio of initial solute concentration, i.e. dissolved solids concentration of solute i in the feedstock solution, to its solid true density. This model assumes co-solidification occurs when the true density of the mixture is reached at the surface.⁵ The true densities of trehalose, pullulan, and trileucine were assumed to be 1580 kg m^{-3} ,⁹ 1850 kg m^{-3} ,⁵ and 1250 kg m^{-3} , respectively. Pluronic F-68 was assumed to have the same true density as trehalose. Leucine was not modelled in this way as it crystallizes and separates from the other excipients.

The volume equivalent diameter at the time of shell formation, d_v , can be predicted for multi-component fully amorphous microparticles, according to,⁵

$$d_v = \sqrt{d_0^2 - \kappa t_{t,mix}} \quad (13)$$

The particle density, ρ_p , may be predicted according to a mass balance,²⁷

$$\rho_p = C_f \left(\frac{d_0}{d_v} \right)^3 \quad (14)$$

where C_f is the total combined solute concentration in the feedstock.

The true density of a solid mixture, $\rho_{t,mix}$, is defined as,⁵

$$\rho_{t,mix} = \frac{1}{\sum_i \frac{Y_i}{\rho_{t,i}}} \quad (15)$$

where Y_i is the mass fraction of component i . If the ratio $\rho_p/\rho_{t,mix}$ is much less than one, the particle is expected to be hollow or wrinkled, or to have a smaller diameter than predicted due to particle contraction after initial solidification. If the ratio is near one, the particle is expected to be spherical and solid, and to have a diameter near the predicted value.

To examine the particle morphology, scanning electron microscopy (SEM) was performed with a field-emission SEM (Zeiss Sigma FESEM, Oberkochen, Germany) using settings of 5000× magnification, working distance ~7 mm, and accelerating voltage 2 kV. An immersion lens (in-lens) detector, which is a type of secondary electron detector, was used in the SEM to provide topographical images. A sputter deposition system (Denton II; Denton Vacuum LLC, Moorestown, NJ, USA) was used prior to imaging to apply a gold coating of ~10 nm to minimize charging. Images were taken immediately after spray drying.

Processing Titer Reduction and Stability Testing

The processing titer reduction was defined as the titer of the initial phage lysate (divided by 100 due to the 1:100 dilution step) minus the titer of the spray-dried phage powder. The titer was measured using spot plaque assays, which are an *in vitro* test of biological activity because they are conducted on the pathogen. To assay the titers of the spray-dried powders, the powders were dissolved in water using a target concentration of 30 mg mL⁻¹. The titer was also measured after room temperature storage for 1 month, in a packaging system described previously.⁴ For trileucine containing formulation, due to the low aqueous solubility, the formulation was allowed to dissolve for approximately five days prior to assay.

Statistics

260 Titer reduction results are given as mean \pm standard deviation based on spot assays performed in triplicate. Statistical comparisons were performed using the Student's t-test at a significance level of 0.05 without assuming equal variance.

RESULTS

Spray Dryer Process Modelling

265 The obtained heat loss constants for use in equation (5) were $\alpha = 4.75 \times 10^{-3} \text{ kW K}^{-1}$ and $\beta = -1.39 \text{ kW}$ ($R^2 = 0.82$) for the spray dryer used in this study. Using these constants, the process model predictions of outlet temperature and outlet water activity are given in Figure 2. As expected, higher inlet temperature and drying gas mass flow rate corresponded to higher outlet temperature and lower outlet water activity. Due to evaporative cooling, higher liquid

270 feed mass flow rate corresponded to lower outlet temperature and higher outlet water activity, as expected. An inlet temperature of 70°C , drying gas flow rate of $8.5 \times 10^{-3} \text{ kg s}^{-1}$, and liquid feed flow rate of $1.7 \times 10^{-5} \text{ kg s}^{-1}$ were used in this study and resulted in a predicted outlet temperature of 49°C and outlet water activity of 0.029. The measured outlet temperature during spray drying experiments matched the process model predictions to

275 within 2°C .

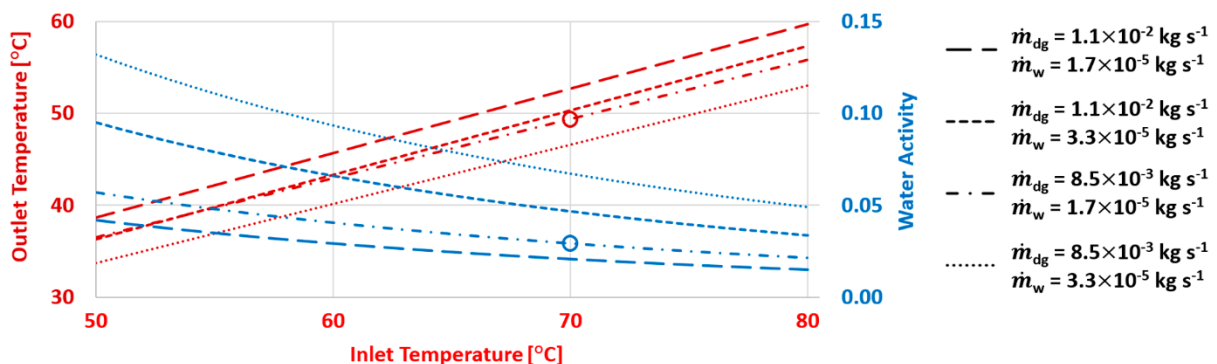
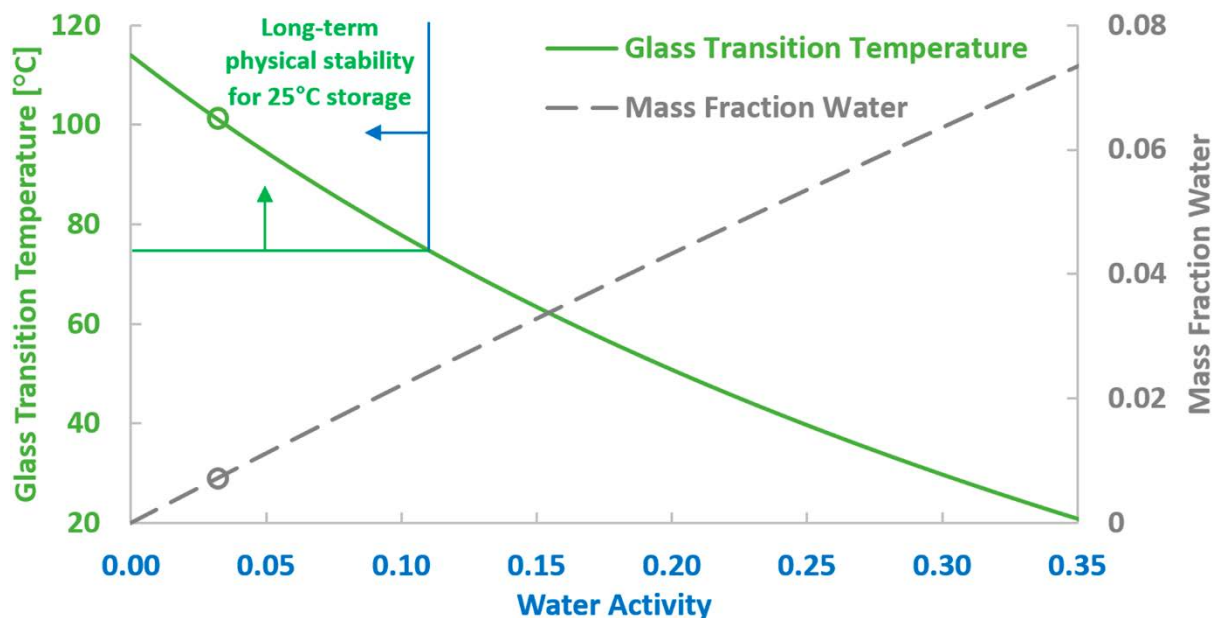


Figure 2: Process model predictions of outlet temperature and outlet water activity for different inlet temperatures, drying gas mass flow rates, and solvent mass flow rates. The chosen conditions are indicated by circles. Full resolution colour image available online.

280 The predicted moisture content and glass transition temperature of trehalose powder for different outlet water activities are given in Figure 3. For the chosen outlet water activity, the outlet moisture content is low enough that a sufficiently high glass transition temperature is expected to be achieved for long-term physical stability with room temperature storage.



285

Figure 3: Mass fraction of water and glass transition temperature of trehalose powder in equilibrium with different spray dryer outlet water activities. The chosen conditions are indicated by circles and are in the region for long-term physical stability, based on a glass transition temperature at least 50°C above the 25°C storage temperature.

290 *Supplemented Phase Diagram*

The developed supplemented phase diagram is given in Figure 4. Long-term physical stability was predicted in terms of retention of amorphous structure for the chosen

processing and storage conditions. Considering that both pullulan and trehalose have high glass transition temperatures (see Introduction), both were also predicted to have long-term physical stability. Good manufacturability was predicted as the glass transition temperature was not approached during processing.

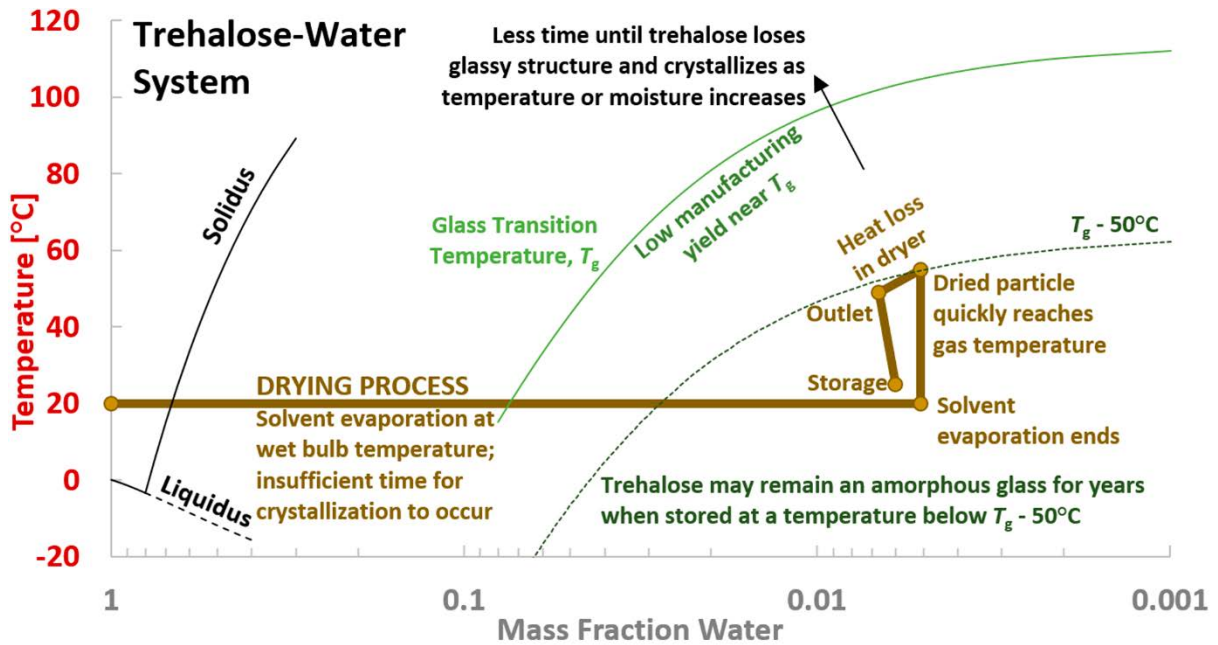


Figure 4: Non-equilibrium supplemented phase diagram for a trehalose-water system.

As expected, Raman spectroscopy confirmed at least 4 months of physical stability for each tested fully amorphous powder, with trehalose, pullulan, pluronic F-68, and trehalose each retaining their amorphous structure.

Microparticle Engineering Models and Particle Morphology

The Péclet number was 1.0 for trehalose, leucine, and trileucine, 4.8 for pluronic F-68, and 18 for pullulan. Consequently, the predicted surface enrichment was 1.2 for trehalose, leucine, and trileucine, 2.2 for pluronic F-68, and 6.3 for pullulan. The microparticle engineering parameter predictions are given for the fully amorphous formulations in Table 1.

Table 1: Microparticle engineering parameter predictions of the evaporation time until solidification begins at the surface, $t_{t,mix}$, volume equivalent diameter at the onset of shell formation, d_v , particle density, ρ_p , and ratio of particle density to true density of the mixture, $\rho_p/\rho_{t,mix}$, for the different tested fully amorphous formulations.

Formulation	$t_{t,mix}$ (ms)	d_v (μm)	ρ_p ($\times 10^3 \text{ kg m}^{-3}$)	$\rho_p/\rho_{t,mix}$
4LLL 100T [∨]	16.5 ± 0.3	3.9 ± 0.2	1.3 ± 0.2	0.83 ± 0.15
20P 100T	14.7 ± 0.3	4.7 ± 0.2	0.8 ± 0.1	0.51 ± 0.06
20P	16.9 ± 0.3	3.7 ± 0.3	0.3 ± 0.1	0.16 ± 0.03
4S 100T [∨]	16.4 ± 0.3	3.9 ± 0.2	1.3 ± 0.2	0.80 ± 0.15
100T	16.6 ± 0.3	3.8 ± 0.2	1.3 ± 0.3	0.83 ± 0.16
20T	19.0 ± 0.4	2.2 ± 0.5	N/A ^δ	N/A ^δ

Notation: LLL = trileucine; P = pullulan; T = trehalose; S = pluronic F-68; preceding number denotes feedstock solute concentration in mg mL^{-1} .

The results are presented as prediction \pm uncertainty estimate, neglecting uncertainty in the material true density and the initial droplet diameter.

Leucine containing formulation was not modelled due to leucine crystallization.

[∨] note that trileucine and pluronic F-68 are surface active, which may cause decreased $t_{t,mix}$, increased d_v , decreased ρ_p , and decreased $\rho_p/\rho_{t,mix}$ predictions relative to the values in this table.

^δ for these cases, uncertainty was too large for a reasonable uncertainty estimate, but nominal values were the same as for 100T.

SEMs of the spray-dried powders containing phage CP30A are presented in Figure 5. The leucine trehalose microparticles appeared to have small leucine crystals near the surface.

Raman spectroscopy confirmed leucine was partially crystalline, while trehalose was fully amorphous. The trileucine trehalose microparticles were wrinkled. A previous study demonstrated that trileucine tends to form wrinkled microparticles when spray-dried with different actives and excipients.¹⁵ Trileucine tends to control the morphology of microparticles as it is typically designed to solidify at the surface prior to the other excipients by using it at a higher saturation level in the liquid feed solution than the other excipients. The pluronic F-68 trehalose microparticles were small and spherical. The pullulan trehalose microparticles were semi-wrinkled, in agreement with the literature for the tested mass fractions,⁵ and appeared to have a smaller diameter than predicted, potentially

associated with the low $\rho_p/\rho_{t,mix}$ value, indicating particle contraction occurred after initial
325 solidification. The pullulan-only microparticles had a very low $\rho_p/\rho_{t,mix}$ value and were
accordingly very collapsed, in agreement with the literature.⁵ The trehalose microparticles
were spherical, as expected.⁵

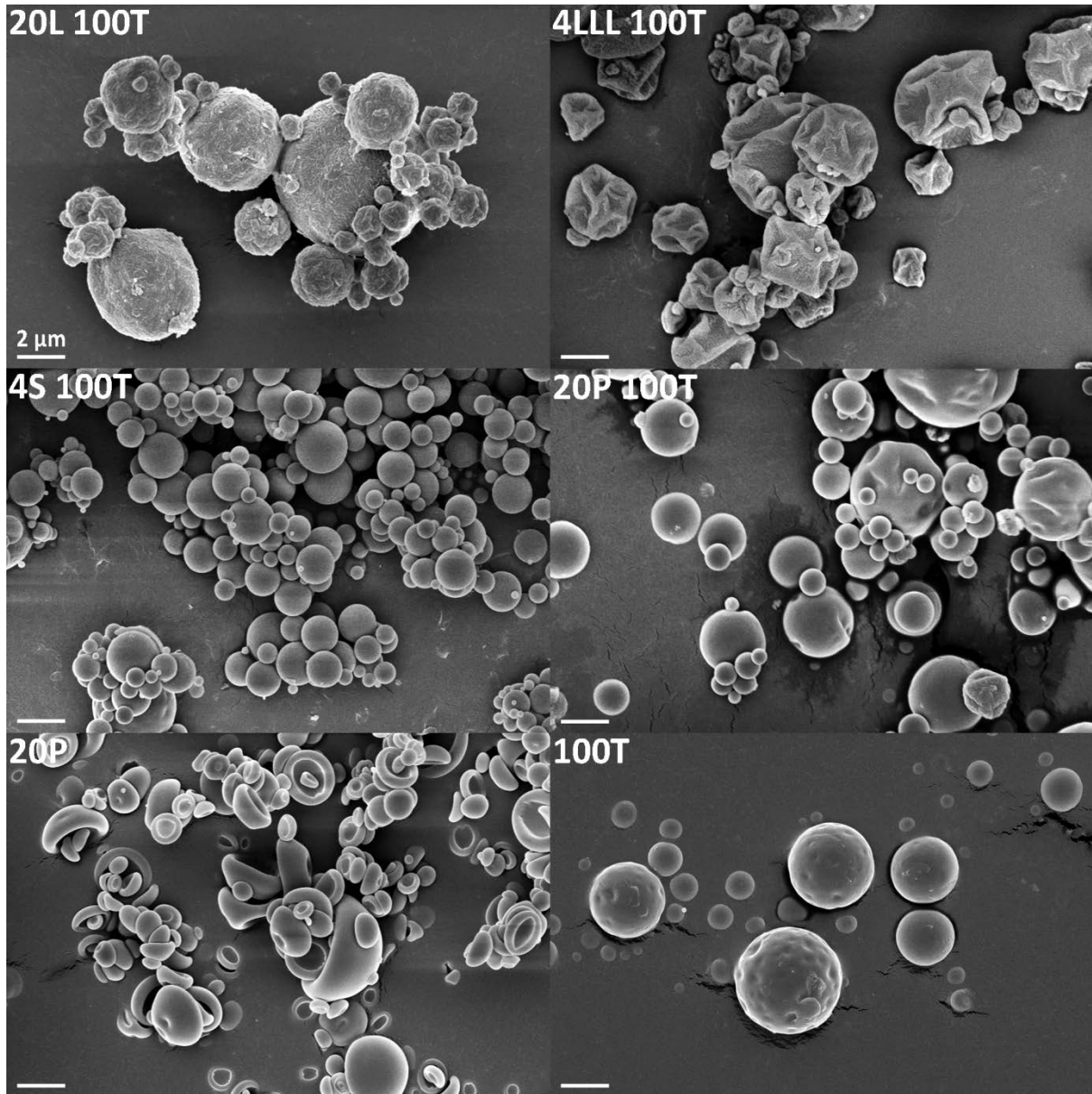


Figure 5: SEMs of phage CP30A powders spray-dried with different excipients. Notation: L =
330 leucine; T = trehalose; LLL = trileucine; S = pluronic F-68 surfactant; P = pullulan; preceding
number denotes feedstock dissolved solids concentration in mg mL^{-1} . 20T microparticles
(not shown) were small ($< 2 \mu\text{m}$) and spherical. Images were taken of the powder

immediately after processing. A change in particle morphology is not expected after 1 month of room temperature storage for the formulations containing trileucine or pullulan

335 based on the high glass transition temperatures of the excipients used. The same magnification was used in all images.

Processing Titer Reduction and Stability Testing

The results of processing phage CP30A by spray drying and storing for 1 month in packaging protecting against humidity intrusion are given in Table 2. The use of trileucine resulted in
340 the least overall titer reduction after processing and 1-month room temperature storage, with a total of only $0.6 \pm 0.1 \log_{10}(\text{PFU mL}^{-1})$ titer reduction, which is a relatively low titer reduction for a biological powder production process.¹³ The use of pullulan with trehalose also outperformed the standard formulation of leucine with trehalose. The use of pluronic F-68 surfactant resulted in much worse stabilization than the use of trileucine, despite the
345 same solids concentration and surface activity, and also resulted in very low manufacturing yield, potentially due to the glass transition temperature being exceeded during the spray drying process. Formulations with trehalose or pullulan alone performed poorly. The use of pullulan alone matched the use of trehalose alone when they were designed to have approximately the same evaporation time until solidification at the surface (see Table 1).
350 The use of a higher solids concentration of trehalose outperformed a lower solids concentration in terms of titer reduction and manufacturing yield.

Table 2: Processing and 1-month room temperature storage titer reductions of phage CP30A powders spray-dried with different formulations.

Formulation	Processing Titer Reduction, $\log_{10}(\text{PFU mL}^{-1})$	Processing + 1 Month Storage Titer Reduction, $\log_{10}(\text{PFU mL}^{-1})$
4LLL 100T	U.A.	0.6 ± 0.1 *
20P 100T	1.0 ± 0.1 * †	1.7 ± 0.1 ***
20L 100T	1.7 ± 0.1 ** ††	1.9 ± 0.1 *
20P	2.4 ± 0.2	N.M.
4S 100T	2.4 ± 0.2	N.M.
100T	2.4 ± 0.1 * †	3.9 ± 0.2
20T	3.3 ± 0.0	N.M.

Notation: LLL = trileucine; T = trehalose; P = pullulan; L = leucine; S = pluronic F-68 surfactant; preceding number denotes feedstock solute concentration in mg mL^{-1}

“U.A.” indicates unsuccessful assay associated with insufficient time given for trileucine to dissolve

“N.M.” indicates not measured

* significantly less ($p < 0.001$) titer reduction, i.e. better biological stabilization, than formulations below in the same column

** significantly less ($p < 0.01$) titer reduction due to processing for 20L 100T than formulations below in the same column

*** significantly less ($p < 0.05$) titer reduction for 20P 100T than 20L 100T after processing and 1 month storage

† significantly less ($p < 0.0025$) titer reduction after processing than after processing and with 1 month storage, indicating loss of biological stability upon storage

†† significantly less ($p < 0.05$) titer reduction after processing than after processing and with 1 month storage, indicating loss of biological stability upon storage

355 DISCUSSION

The objective of this research was to develop a stable anti-*Campylobacter* phage powder with minimal titer reduction due to spray drying and room temperature storage through the use of process modelling, a supplemented phase diagram, and microparticle engineering.

360 Generally, processing losses of greater than $1 \log_{10}(\text{PFU mL}^{-1})$ would lead to more expensive products which could make them unsuitable for developing countries. In order to protect against desiccation stress and the corresponding phage inactivation, the use of amorphous glass stabilizers trileucine and pullulan was tested and compared to the commonly used crystalline shell former leucine.

Leucine was shown to be partially crystalline and thus could not provide adequate glass
365 stabilization to counter desiccation stress. Indeed, there is no glass stabilization within a
crystal, and phages located within a forming crystal may be broken apart or expelled.

The stabilization achieved with amorphous shell formers pullulan or trileucine with
trehalose outperformed leucine with trehalose, as hypothesized, and produced flowable
powders. This was a novel finding as, to the authors' knowledge, neither pullulan nor
370 trileucine have been spray-dried with phages before. The use of pullulan or trehalose alone
did not provide the same extent of biological stabilization as did their combination. This is
perhaps related to better stabilization occurring with a core-shell microparticle structure, or
with the earlier co-solidification at the surface when used in combination, which would
decrease the fraction of phages that would otherwise be exposed to the drying gas and
375 associated desiccation stress as the droplet shrinks. The latter was supported by the results
showing that using trehalose at a higher initial dissolved solids concentration (100 mg mL^{-1}),
for which solidification occurs earlier and may prevent as many phages from reaching the
surface, provided better, albeit insufficient, biological stabilization than using trehalose at a
lower initial dissolved solids concentration (20 mg mL^{-1}). This was also supported by results
380 showing that the same level of biological stabilization was provided by pullulan-only as by
trehalose-only when they experienced approximately the same evaporation time until
solidification at the surface (see Table 1) and hence approximately the same predicted
diameter and predicted phage surface concentration at initial shell solidification. This
happened despite different solids concentrations, i.e. biologic-to-glass stabilizer ratios. The

385 proposed particle formation mechanisms and their relation to biological stabilization are described in more detail in Figure 6 and in the footnote[§].

[§] A droplet emitted from the atomizer is assumed to initially be well-mixed in terms of the excipients being evenly distributed within the droplet, while the phages are assumed to be randomly distributed. "A": trileucine is surface-active and near saturation initially and forms an amorphous shell with small amounts of trehalose early, before all phages are present at the surface. The mainly trileucine shell folds, potentially since it is thin and rubbery; the mainly trehalose interior has yet to solidify. The shell potentially maintains the same surface area upon folding and prevents phages from reaching the surface. "B": the crumpled appearance is controlled by the folded shell. The interior later solidifies into a glass from a highly viscous solution due to further desiccation. "C": pullulan enriches at the surface due to high molecular mass and forms a viscous amorphous shell that contains small amounts of trehalose; the shell contracts, causing phages to recede with the surface, and desiccates until a glassy mixture of pullulan and trehalose is present at the surface. "D": the surface is mainly pullulan, with some trehalose that may have prevented shell deformation. The interior is mainly trehalose with some pullulan. "E": nucleation at the surface results in small leucine crystals that eventually become close enough and large enough to form a shell. Trehalose and remaining leucine eventually solidify. "F": phages could be expelled from crystals, be damaged by inter-crystal forces, or inhibit crystallization. Small crystals are at the surface of the microparticles. The interior is primarily trehalose and may contain voids. "G": pullulan enriches near the surface and solidifies there. The thin shell is moderately rigid due to a high glass transition temperature and may easily deform and contract as it is not hindered by a trehalose interior. "H": there is no trehalose glass stabilizer or void space in the interior. "I": surfactant may form a film that recedes but does not adequately stabilize the phages. "J": small cohesive spherical microparticle with phages near or on the surface where they are not adequately stabilized by the low glass transition temperature surfactant. "K": small cohesive solid spherical microparticle formed. There is a high chance that phages reside on the surface. "L": same as "K" except that a very small microparticle results and there is a very high chance that phages reside on surface. Void space is not shown in the schematic and may be possible in many cases. Note that there is likely a radial distribution of each excipient within the drying droplet rather than complete separation of excipients.

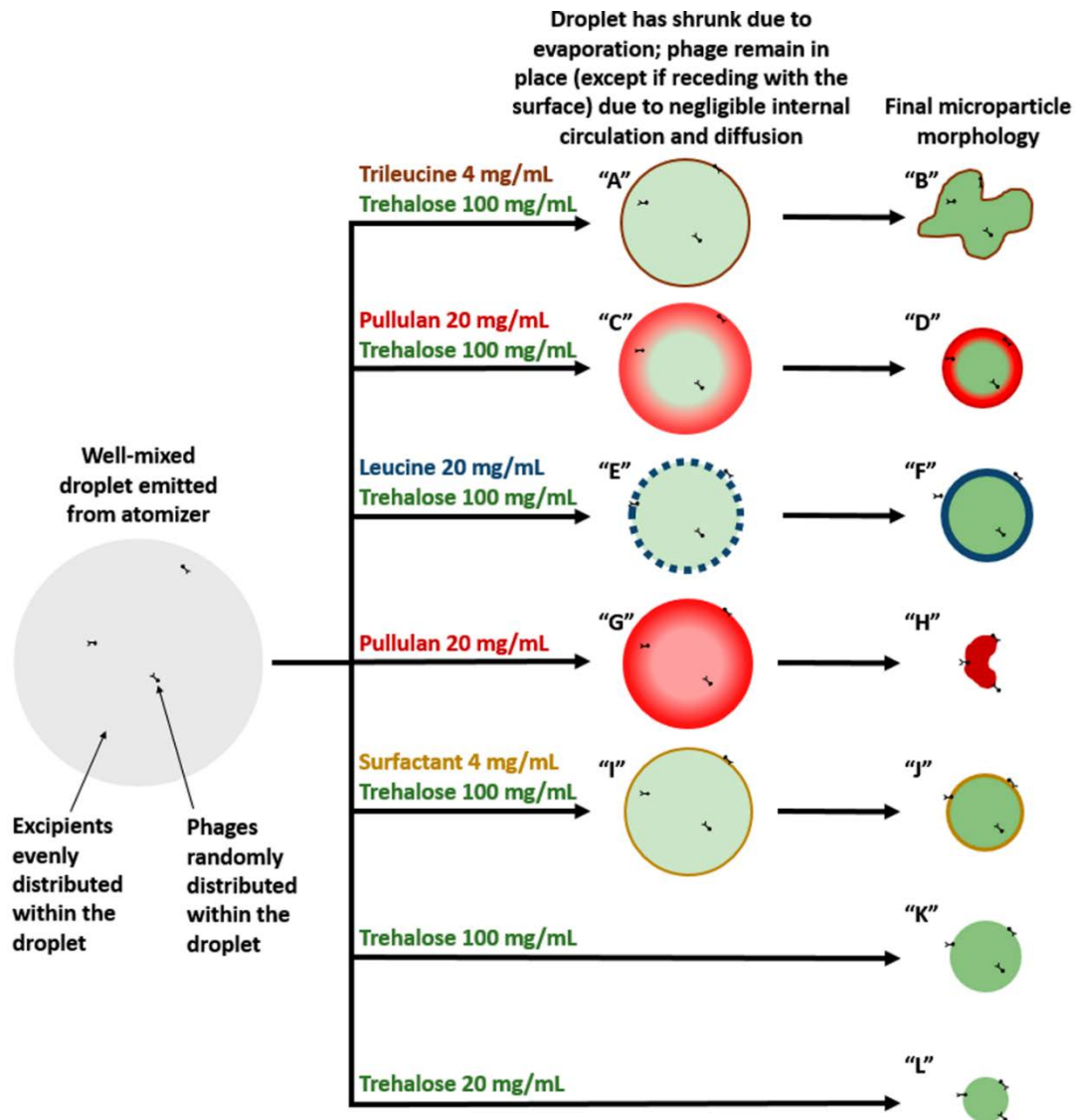


Figure 6: Schematic of the particle formation mechanisms for the different tested

formulations and their relationship to phage distribution and stabilization. The best

390 performing to worst performing formulations are from top to bottom. Descriptions of the

particle formation processes are available in the footnote. Full resolution colour image

available online.

To our knowledge, this is the first study in which phages have been spray-dried with

trileucine, and excellent biological stabilization was observed, with an overall titer reduction

395 of $0.6 \pm 0.1 \log_{10}(\text{PFU mL}^{-1})$ due to formulation, spray drying, 1-month dry room

temperature storage, and dissolving the powder in water for plaque assay. Based on microparticle formation calculations, trileucine is expected to form a very thin amorphous shell at the surface early in the drying process that provides glass stabilization to the phages and prevents the phages from reaching the surface and being exposed to desiccation stress.

400 The shell may fold because it is thin and has a high flexibility^{11,32} in a rubbery, deformable state when initially formed at a high moisture content; after drying further the trileucine will progress to a glassy phase. Despite a similar surface activity, the pluronic F-68 surfactant did not provide the same level of stabilization as trileucine. This is perhaps due to poor biologic stabilization provided by the surfactant, which may be associated with its low glass
405 transition temperature resulting in a suitable glassy phase not being formed after drying. The better stability using trileucine rather than surfactant indicated the importance of using a high glass transition temperature amorphous shell former rather than a low glass transition temperature amorphous shell former. The greater stabilization with trileucine as compared to pullulan may be related to the smaller molecular mass of trileucine, allowing
410 the glass to more closely interact with the biologic, or to the surface activity, better preventing the phages from reaching the surface during drying.

Phages have previously been stabilized in pullulan trehalose films.¹⁶ To our knowledge, this is the first time pullulan trehalose microparticles have been used to stabilize biologics. This combination showed excellent biologic stabilization potential, outperforming the standard
415 leucine trehalose combination that is commonly proposed for spray drying phages. Other high glass transition temperature polysaccharides than pullulan may also be suitable for glass stabilization near the surface of spray-dried microparticles.

Both novel successful spray-dried formulations, trileucine with trehalose, and pullulan with trehalose, were fully amorphous as opposed to the traditional crystalline shell-amorphous

420 core system, leucine with trehalose. The amorphous shell platform for stabilizing biologics developed in this work consists of the use of a high glass transition temperature excipient that solidifies to an amorphous phase at the surface early in the spray drying process due to any combination of high initial dissolved solids concentration, high surface activity, or high molecular mass (associated with slow diffusion and hence high surface enrichment). In this 425 study, the best stabilization was obtained using trileucine as an amorphous shell former, an excipient with intermediate molecular mass, high surface activity, and low solubility.

In summary, the use of processing modelling, microparticle engineering, and a supplemented phase diagram allowed for expedited design of physically stable spray-dried powder capable of stabilizing biological material with no iterations necessary to find suitable 430 processing conditions. Based on data presented here, the use of a high glass transition temperature amorphous shell former that solidifies at the surface early in the drying process is recommended for glass stabilization of spray-dried phage CP30A against the main inactivating factor, desiccation at the surface of the drying microparticles. Indeed, fully amorphous formulation using trileucine (dry glass transition temperature $\sim 104^{\circ}\text{C}$) or 435 pullulan (dry glass transition temperature $\sim 261^{\circ}\text{C}$) as shell-forming excipients and trehalose as a bulk glass stabilizer are promising alternatives to the standard crystal leucine shell and amorphous trehalose interior formulation for the development of stable spray-dried phage powders. With the fully amorphous approach, at least 1-month dry room temperature storage stability of active anti-*Campylobacter* phage CP30A in a flowable powder was 440 achieved. The proposed amorphous shell platform is expected to be useful for the stabilization of other biologics that generally tend to concentrate on the surface of spray-dried microparticles and may have a variety of applications in the biomedical engineering and other industries.

ACKNOWLEDGEMENTS

445 NC thanks the Killam Trusts, the Natural Sciences and Engineering Research Council of
Canada, Alberta Innovates, and the University of Alberta for scholarship funding. This work
was financially supported by the Biotechnology and Biological Sciences Research Council
[grant number BB/P02355X/1] (United Kingdom). The funding source had no role in study
design, collection, analysis, or interpretation of data, writing the article, or in decision to
450 submit the article for publication.

REFERENCES

1. Anandharamakrishnan, C. and S. Padma Ishwarya. Spray Drying Techniques for Food
Ingredient Encapsulation. Chichester: John Wiley & Sons, Inc., 2015.
2. Broadhead, J., S.K. Edmond Rouan, and C.T. Rhodes. The spray drying of pharmaceuticals.
455 Drug. Dev. Ind. Pharm. 18:1169-1206, 1992.
3. Carrigy, N.B. and R. Vehring. "Engineering stable spray-dried biologic powder for
inhalation." In: Pharmaceutical Inhalation Aerosol Technology, Third Edition, edited by A.J.
Hickey and S. da Rocha. Boca Raton: CRC Press, 2019, pp. 291-326.
4. Carrigy, N.B., L. Liang, H. Wang, S. Kariuki, T.E. Nagel, I.F. Connerton, and R. Vehring.
460 Spray-dried anti-*Campylobacter* bacteriophage CP30A powder suitable for global
distribution without cold chain infrastructure. Int. J. Pharm. 569:118601, 2019.
5. Carrigy, N.B., M. Ordoubadi, Y. Liu, O. Melhem, D. Barona, H. Wang, L. Milburn, C.A.
Ruzycski, W.H. Finlay, and R. Vehring. Amorphous pullulan trehalose microparticle platform
for respiratory delivery. Int. J. Pharm. 563:156-168, 2019.

- 465 6. Chen, T., A. Fowler, and M. Toner. Literature review: supplemented phase diagram of the trehalose-water binary mixture. *Cryobiology*. 40:277-282, 2000.
7. di Stefano, F. Pullulan as release enhancer for controlled release capsular device: performance assessment and preparation methods. M.Sc. Thesis, Department of Chemistry, Materials and Chemical Engineering, Politecnico di Milano, Milan, Italy. 2017.
- 470 8. Feng, A.L., M.A. Boraey, M.A. Gwin, P.R. Finlay, P.J. Kuehl, and R. Vehring. Mechanistic models facilitate efficient development of leucine containing microparticles for pulmonary drug delivery. *Int. J. Pharm.* 409:156-163, 2011.
9. Grasmeijer, N., H.W. Frijlink, and W.L.J. Hinrichs. Model to predict inhomogeneous protein-sugar distribution in powders prepared by spray drying. *J. Aerosol Sci.* 101:22-33,
475 2016.
10. Hancock, B.C., S.L. Shamblin, and G. Zografi. Molecular mobility of amorphous pharmaceutical solids below their glass transition temperatures. *Pharm. Res.* 12:799-806, 1995.
11. Hasegawa, T., J. Umemura, and N. Yamada. Characterization of thin cast films of a
480 trileucine-induced lipid by infrared multiple-angle incidence resolution spectrometry. *J Mol. Struct.* 735-736:63-67, 2005.
12. He, X., L. Pei, H.H.Y. Tong, and Y. Zheng. Comparison of spray freeze drying and the solvent evaporation method for preparing solid dispersions of baicalein with pluronic F68 to improve dissolution and oral bioavailability. *AAPS PharmSciTech.* 12:104-113, 2011.

- 485 13. Hoe, S., D.D. Semler, A.D. Goudie, K.H. Lynch, S. Matinkhoo, W.H. Finlay, J.J. Dennis, and R. Vehring. Respirable bacteriophages for the treatment of bacterial lung infections. *J. Aerosol Med. Pulm. Drug Deliv.* 26:317-335, 2013.
14. Hoe, S., J.W. Ivey, M.A. Boraey, A. Shamsaddini-Shahrbabek, E. Javaheri, S. Matinkhoo, W.H. Finlay, and R. Vehring. Use of a fundamental approach to spray-drying formulation
490 design to facilitate the development of multi-component dry powder aerosols for respiratory drug delivery. *Pharm. Res.* 31:449-465, 2014.
15. Lechuga-Ballesteros, D., C. Charan, C.L.M. Stults, C.L. Stevenson, D.P. Miller, R. Vehring, V. Tep, and M.C. Kuo. Trileucine improves aerosol performance and stability of spray-dried powders for inhalation. *J. Pharm. Sci.* 97:287-302, 2008.
- 495 16. Leung, V., A. Szewczyk, J. Chau, Z. Hosseinidoust, L. Groves, H. Hawsawi, H. Anany, M.W. Griffiths, M.M. Ali, C.D.M. Filipe. Long-term preservation of bacteriophage antimicrobials using sugar glasses. *ACS Biomater. Sci. Eng.* 4:3802-3808, 2018.
17. Masters, K. *Spray Drying: An Introduction to Principles, Operational Practice and Applications*. London: Leonard Hill Books, 1972.
- 500 18. Nishinari, K., K. Kohyama, P.A. Williams, G.O. Phillips, W. Burchard, and K. Ogino. Solution properties of pullulan. *Macromolecules.* 24:5590-5593, 1991.
19. O'Reilly, C.E., P. Jaron, B. Ochieng, A. Nyaguara, J.E. Tate, M.B. Parsons, C.A. Bopp, K.A. Williams, J. Vinjé, E. Blanton, K.A. Wannemuehler, J. Vulule, K.F. Laserson, R.F. Breiman, D.R. Feikin, M.A. Widdowson, and E. Mintz. Risk factors for death among children less than 5
505 years old hospitalized with diarrhea in rural western Kenya, 2005-2007: a cohort study. *PLoS Med.* 9:e1001256, 2012.

20. Roe, K.D. and T.P. Labuza. Glass transition and crystallization of amorphous trehalose-sucrose mixtures. *Int. J. Food Prop.* 8:559-574, 2005.
21. Rumble, J.R. *CRC Handbook of Chemistry and Physics*, 98th Edition. Boca Raton: CRC Press, 2018.
22. Schwartzbach, H. Achieving aseptic drying with spray drying technologies. *Pharmaceutical Technology Europe*. 23: 90-92, 2011.
23. Siew, A. Exploring the use of aseptic spray drying in the manufacture of biopharmaceutical injectables. *Pharmaceutical Technology*. 40:24-27, 2016.
24. Singh, R.S. and G.K. Saini. "Biosynthesis of pullulan and its applications in food and pharmaceutical industry." In: *Microorganisms in Sustainable Agriculture and Biotechnology*, edited by T. Satyanarayana, B.N. Johri, and A. Prakash. Dordrecht: Springer Science+Business Media B.V., 2012, pp. 509-553.
25. Teekamp, N., Y. Tian, J.C. Visser, P. Olinga, H.W. Frijlink, H.J. Woerdenbag, and W.L.J. Hinrichs. Addition of pullulan to trehalose glasses improves the stability of β -galactosidase at high moisture contents. *Carbohydr. Polym.* 176:374-380, 2017.
26. Vandenheuvel, D., J. Meeus, R. Lavigne, and G. van den Mooter. Instability of bacteriophage in spray-dried trehalose powders is caused by crystallization of the matrix. *Int. J. Pharm.* 472:202-205, 2014.
27. Vehring, R. Pharmaceutical particle engineering via spray drying. *Pharm. Res.* 25:999-1022, 2008.
28. Vehring, R., W.R. Foss, and D. Lechuga-Ballesteros. Particle formation in spray drying. *J. Aerosol Sci.* 38:728-746, 2007.

29. Walsh, G. Biopharmaceutical benchmarks 2014. *Nat. Biotechnol.* 32:992-1000, 2014.
- 530 30. Walters, R.H., B. Bhatnagar, S. Tchessalov, K.I. Izutsu, K. Tsumoto, and S. Ohtake. Next generation drying technologies for pharmaceutical applications. *J. Pharm. Sci.* 103:2673-2695, 2014.
31. Wang, H., M.A. Boraey, L. Williams, D. Lechuga-Ballesteros, and R. Vehring. Low-frequency shift dispersive Raman spectroscopy for analysis of respirable dosage forms. *Int. J. Pharm.* 469:197-205, 2014.
- 535 32. Yamada, N., T. Komatsu, H. Yoshinaga, K. Yoshizawa, S. Edo, and M. Kunitake. Self-supporting elastic film without covalent linkages as a hierarchically integrated β -sheet assembly. *Angew. Chem. Int. Ed.* 42:5496-5499, 2003.